Beyond non-integer Hill coefficients: A novel approach to analyzing binding data, applied to Na^+-driven transporters

Silvia Ravera,[1] Matthias Quick,[2] Juan P. Nicola,[1] Nancy Carrasco,[1] and L. Mario Amzel[3]

[1]Department of Cellular and Molecular Physiology, Yale University School of Medicine, New Haven, CT 06510
[2]Center for Molecular Recognition, Columbia University College of Physicians and Surgeons, New York, NY 10032
[3]Department of Biophysics and Biophysical Chemistry, Johns Hopkins University School of Medicine, Baltimore, MD 21205

Prokaryotic and eukaryotic Na^+-driven transporters couple the movement of one or more Na^+ ions down their electrochemical gradient to the active transport of a variety of solutes. When more than one Na^+ is involved, Na^+-binding data are usually analyzed using the Hill equation with a non-integer exponent n. The results of this analysis are an overall K_d-like constant equal to the concentration of ligand that produces half saturation and n, a measure of cooperativity. This information is usually insufficient to provide the basis for mechanistic models. In the case of transport using two Na^+ ions, an $n < 2$ indicates that molecules with only one of the two sites occupied are present at low saturation. Here, we propose a new way of analyzing Na^+-binding data for the case of two Na^+ ions that, by taking into account binding to individual sites, provides far more information than can be obtained by using the Hill equation with a non-integer coefficient: it yields pairs of possible values for the Na^+ affinities of the individual sites that can only vary within narrowly bounded ranges. To illustrate the advantages of the method, we present experimental scintillation proximity assay (SPA) data on binding of Na^+ to the Na^+/I^- symporter (NIS). SPA is a method widely used to study the binding of Na^+ to Na^+-driven transporters. NIS is the key plasma membrane protein that mediates active I^- transport in the thyroid gland, the first step in the biosynthesis of the thyroid hormones, of which iodine is an essential constituent. NIS activity is electrogenic, with a 2:1 Na^+/I^- transport stoichiometry. The formalism proposed here is general and can be used to analyze data on other proteins with two binding sites for the same substrate.

The Journal of General Physiology

INTRODUCTION

Membrane transport proteins serve a key function in living cells by mediating the transport of many different solutes, such as ions, nutrients, and neurotransmitters across biological membranes. Numerous pathological conditions—cystinuria (Fotiadis et al., 2013), glucose–galactose malabsorption (Wright, 2013), hypothyroidism caused by iodide transport defects (Levy et al., 1998; De la Vieja et al., 2007; Paroder-Belenitsky et al., 2011; Portulano et al., 2014)—result from impairments in the function of molecules of this class. Membrane transporters also play a crucial role in the delivery of chemotherapeutic agents and internal radiation (Klutz et al., 2011; Ho et al., 2013) to cancer cells.

Many prokaryotic and eukaryotic transporters exploit the electrochemical gradient of Na^+ to translocate their substrates across the membrane. Of those, a significant fraction binds and transports more than one Na^+ ion per transport cycle (Caplan et al., 2008; Shi et al., 2008; Abramson and Wright, 2009). Binding assays using a radiotracer in scintillation proximity assays (SPAs) have become a routine procedure for investigating the function of detergent-solubilized transport proteins and, critically, for determining the substrate-binding constants of purified transporters (Pirch et al., 2002; Berry and Price-Jones, 2005; Quick and Javitch, 2007; Harder and Fotiadis, 2012; Khafizov et al., 2012; Zhou et al., 2014).

Conventionally, when more than one Na^+ is involved, SPA data are analyzed using the Hill equation (Hill, 1910, 1913; Weiss, 1997; Goutelle et al., 2008) with a non-integer exponent n:

$$f_n = \left[Na^+\right]^n \Big/ \left(K_d^n + \left[Na^+\right]^n\right), \quad (1)$$

where f_n is the fraction of transporter molecules that are occupied by Na^+, and K_d is an apparent microscopic dissociation constant. Cases with $n > 1$ are instances of positive cooperativity, and the resulting curves for f_n versus $[Na^+]$ are sigmoidal; the K_d value yields the $[Na^+]$ at half-saturation. This equation, however, does not describe a true equilibrium situation: there is no real binding reaction that can lead to this expression, as it would have a fractional stoichiometric coefficient. In the case

Correspondence to Nancy Carrasco: nancy.carrasco@yale.edu; or L. Mario Amzel: mamzel@jhmi.edu

Juan P. Nicola's current address is Departamento de Bioquímica Clínica, Facultad de Ciencias Químicas, Universidad Nacional de Córdoba, Córdoba 5000, Argentina.

Abbreviations used in this paper: NIS, Na^+/I^- symporter; SPA, scintillation proximity assay.

The Rockefeller University Press $30.00
J. Gen. Physiol. Vol. 145 No. 6 555–563
www.jgp.org/cgi/doi/10.1085/jgp.201511365

of two binding sites, for example, a fractional Hill coefficient indicates that proteins with only one site occupied represent a significant fraction of the molecules in equilibrium, especially at low [Na^+].

Here, we propose a novel way of analyzing SPA data obtained from experiments with transporters that bind Na^+ at two sites. The method is exemplified by analyzing experimental SPA data from the Na^+/I^- symporter (NIS). This approach, which takes into account binding to individual sites, provides information not accessible with the traditional Hill equation analysis.

MATERIALS AND METHODS

Protein purification

293-H cells grown in suspension were transduced with a lentiviral vector containing a rat NIS cDNA construct with an HA tag at the N terminus and a His_8 tag and a streptavidin-binding protein (IBA GmbH) tag at the C terminus. I^- transport levels were comparable to those in FRTL-5 cells, a line of rat thyroid–derived cells that express NIS endogenously (Dai et al., 1996). A membrane fraction prepared from 293 cells was solubilized with 40 mM *n*-dodecyl-β-D-maltopyranoside (DDM; Anatrace) and purified via Strep-Tactin affinity chromatography. The S353A/T354A NIS mutant was expressed and purified using the same procedures.

Binding experiments

Binding experiments were performed using the SPA technique (Quick and Javitch, 2007). Affinity-purified NIS (WT or mutant) was bound to Cu^{2+} chelate YSi scintillation SPA beads (PerkinElmer) via the C-terminal His_8 tag. 250 µg SPA beads was used per assay, in a volume of 100 µl. Experiments consisted of competing bound $^{22}Na^+$ with cold Na^+ at the specified concentrations. The assay buffer consisted of 100–600 mM Tris/Mes, pH 7.5, 20% glycerol, 0–500 mM NaCl (equimolar replacement with Tris/Mes), 1 mM TCEP, and 0.1% DDM with 250 ng of affinity-purified NIS. [^{22}Na]Cl (1,017 mCi/mg; PerkinElmer) and the indicated concentrations of cold NaCl were added to the bead solution simultaneously with the protein. Nonspecific binding was determined in the presence of 800 mM imidazole. All binding assays were performed in white-walled, clear-bottomed 96-well plates and quantitated in a photomultiplier (Wallac; PerkinElmer) tube counter (MicroBeta; PerkinElmer) after overnight equilibration.

Analysis of NIS SPA data

All readings were background-subtracted and then normalized using the following relation:

$$f_x = C_x - C_{500}/C_0 - C_{500},$$

where f_x is the fraction of NIS molecules for which the bound $^{22}Na^+$ has been displaced by cold Na^+ at a [Na^+] = X; and C_0, C_X, and C_{500} are the counts per minute at cold [Na^+] = 0, [Na^+] = X, and [Na^+] = 500 mM.

RESULTS AND DISCUSSION

Non-integer Hill coefficients

The equation proposed by Hill (Hill, 1910, 1913; Dahlquist, 1978; Weiss, 1997; Goutelle et al., 2008) can be written as

$$Y = K_a \cdot [L]^n / \left(1 + K_a \cdot [L]^n\right),$$

and can be considered to represent the equilibrium for the reaction

$$P + nL \rightleftharpoons PL_n \text{ with } K_a = [PL_n]/[P][L]^n,$$

"where K_a is the equilibrium constant and n is a whole number > 1" (Hill, 1913), and Y is the fraction of protein molecules that have n ligands bound.

This reaction and its associated equilibrium constant imply that the protein (P) has n binding sites, and the ligand (L) must bind to the n sites simultaneously: binding of L to a single site of the protein does not take place. The exponent in this equation is called the Hill coefficient.

In many cases, a better fit to the experimental data can be achieved by using a non-integer Hill coefficient, yielding the equation,

$$f_n = [L]^n / \left(K_d^n + [L]^n\right).$$

Unfortunately, this equation does not represent an actual reaction; it just says that L can bind to one site and that binding to one site affects the affinity of the other site for L. A value of $n > 1$ indicates positive cooperativity; an $n < 1$ indicates negative cooperativity.

A more general case would be one in which the protein has two nonequivalent sites and L can bind to either site first and then bind to the other. The two sites will, in general, have different affinities for the ligand, and the affinity for binding to a second site may be enhanced (positive cooperativity) or reduced (negative cooperativity) when the other site is already occupied. The reaction scheme for the general case involving two sites, A and B, is represented in Fig. 1, where $K_{a,A}$ and $K_{a,B}$ are the association constants for the binding of L to the empty protein, $K_{a,A-B}$ is the association constant for binding L to site B when site A is occupied, and $K_{a,B-A}$ is the association

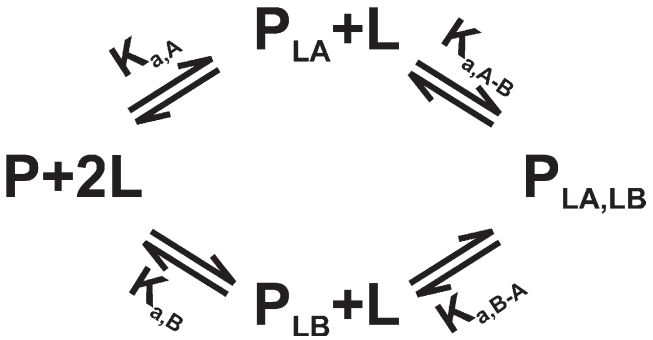

Figure 1. Binding of a ligand L to a protein P with two cooperative binding sites (sites A and B). The association constants for the empty protein are $K_{a,A}$ and $K_{a,B}$, and those for binding of the second ligand are $K_{a,A-B}$ and $K_{a,B-A}$.

constant for binding L to site A when site B is occupied. Note that only three of the four constants are needed because the upper and the lower paths lead to the same species, and therefore $K_{a,A} \cdot K_{a,A-B} = K_{a,B} \cdot K_{a,B-A}$. Introducing ϕ, a unitless enhancement/reduction factor, we can write $K_{a,A-B} = K_{a,B} \cdot \phi$ and $K_{a,B-A} = K_{a,A} \cdot \phi$. For positive cooperativity, $\phi > 1$, and $\phi < 1$ corresponds to negative cooperativity ($\phi = 1$ means independent sites).

The fraction of doubly occupied molecules can be written as

$$f_{2L} = K_{a,A}K_{a,B}\phi[L]^2 \Big/ \left\{1 + \left(K_{a,A} + K_{a,B}\right)[L] + K_{a,A}K_{a,B}\phi[L]^2\right\}, \tag{2a}$$

and the fraction of singly occupied molecules as

$$f_{1L} = \left(K_{a,A} + K_{a,B}\right)[L] \Big/ \left\{1 + \left(K_{a,A} + K_{a,B}\right)[L] + K_{a,A}K_{a,B}\phi[L]^2\right\}. \tag{2b}$$

Introducing the new constants

$$K_p = K_{a,A} + K_{a,B} \tag{3}$$

$$K_x = K_{a,A} \cdot K_{a,B} \cdot \phi \tag{4}$$

yields

$$f_{2L} = K_x[L]^2 \Big/ \left\{1 + K_p[L] + K_x[L]^2\right\} \tag{5a}$$

and

$$f_{1L} = K_p[L] \Big/ \left\{1 + K_p[L] + K_x[L]^2\right\}. \tag{5b}$$

(The sum of Eqs. 5a and 5b is similar to the Adair equation (Adair et al., 1925) but subjected to the conditions given by Eqs. 3 and 4.)

The normalized signal from an experimental measurement sig(L) is given by

$$sig(L) = sr \cdot f_{1L} + f_{2L}, \tag{6}$$

where *sr* is the ratio of the signal when one L is bound to that when two L's are bound.

The values of K_p and K_x can be obtained by a least-squares fit of normalized experimental data. Eqs. 3 and 4 can then be used to solve for $K_{a,A}$ and $K_{a,B}$ as a function of ϕ. This yields a quadratic equation with solutions

$$K_{a,A \text{ or } B} = \frac{1}{2}\left\{K_p \pm \left(K_p^2 - \frac{4K_x}{\phi}\right)^{\frac{1}{2}}\right\}, \tag{7a}$$

where we choose the plus sign for $K_{a,A}$ and the minus sign for $K_{a,B}$. Because $K_{a,A}$ and $K_{a,B}$ must be real numbers, the expression within the square root "*sq*"

$$sq = K_p^2 - \frac{4K_x}{\phi} \tag{7b}$$

or

$$sq = K_{a,A}^2 + K_{a,B}^2 + 2K_{a,A}K_{a,B} - \frac{4K_{a,A}K_{a,B}}{\phi} \tag{7c}$$

must be positive.

Three cases have to be considered: $\phi = 1$, $\phi > 1$, and $\phi < 1$. The case $\phi = 1$ corresponds to two independent sites (no cooperativity). If $sq = 0$, $K_{a,A} = K_{a,B} = 1/2\ K_p$ and corresponds to two independent identical sites; otherwise, $K_{a,A} > K_{a,B}$.

The case $\phi > 1$ corresponds to positive cooperativity. The condition $sq = K_p^2 - 4K_x/\phi > 0$, which is equivalent to $K_p^2 > 4K_x/\phi$, defines a minimum value of $\phi_{min,p} = 4K_x/K_p^2$, such that $\phi_{min,p} \le \phi < \infty$. In contrast, the case $\phi < 1$ corresponds to negative cooperativity. The condition $sq = K_p^2 - 4K_x/\phi > 0$ or $K_p^2 > 4K_x/\phi$ also defines a minimum value of $\phi_{min,n} = 4K_x/K_p^2$, but in this case, $\phi_{min,p} \le \phi < 1$.

In both cases, when $\phi = \phi_{min}$, $sq = 0$; therefore, $K_{a,A} = K_{a,B} = 1/2\,K_p$. A symmetrical homodimer, for example, may correspond to this case if the single sites can bind independently, but once a site is occupied, the affinity for the second site is enhanced/reduced.

In the case of positive cooperativity, there is another limiting case. It corresponds to the situation where ϕ is very large, making $K_{a,A}$ approach K_p and $K_{a,B}$ approach 0 (from Eq. 7a). This case corresponds to absolute sequential binding (i.e., the ligand does not bind to site B unless site A is already occupied).

After the values of K_p and K_x are obtained by fitting the experimental data, combinations of values of $K_{a,A}$ and $K_{a,B}$ can be obtained as a function of the allowed values of ϕ. Although the information obtained is only a range of possible values for the affinities of sites A and B of the empty protein for the ligand, $1/2\,K_p \le K_{a,A} \le K_p$ and $0 \le K_{a,B} \le 1/2\,K_p$, with $K_{a,B} = K_p - K_{a,A}$.

This analysis provides more information than just the single value that is obtained from the Hill equation using non-integer exponents. Furthermore, the values of $K_{a,A}$, $K_{a,B}$, and $K_{a,B} \cdot \phi \left(= K_x/K_{a,A}\right)$ are constrained by Eqs. 3 and 4 and the conditions imposed by Eq. 7. In addition, the formulation corresponds to a well-defined binding mechanism. (The dissociation constant, obtained by computing $K_x^{-1/2}$, is similar to the K_d obtained from the Hill equation.) One issue that may seem puzzling is that $K_{a,B}$ approaches zero (and $K_{d,B}$ approaches ∞) as $K_{a,A}$ approaches K_p. Why does it still correspond to a two-site situation? The answer is simple. Both $K_{a,B}$ and ϕ are a function of $(K_p - K_{a,A})$; $K_{a,B}$ is directly proportional and ϕ is inversely proportional, such that $K_{a,B} \cdot \phi = K_x/K_{a,A}$. That is, as $K_{a,B}$ approaches zero, $K_{a,B} \cdot \phi$ remains bound, and the second site has a finite dissociation constant when site A is occupied. Because $K_{a,A}$ varies only within a factor of 2, $K_{a,B} \cdot \phi$ also varies within a factor of 2.

Because the equations were derived as a function of [L], the concentration of free ligand, they work directly in cases in which [L] is very close to L_{added}, the concentration of ligand added at each experimental point. SPA, in which the amount of protein is much less than the amount of ligand, and fluorescence measurements performed with concentration of protein [P] << K_d satisfy this condition.

In the case of SPA experiments with ^{22}Na (L = Na^+), the transporter with two Na^+ ions bound and the two species with one Na^+ bound all produce a signal. Because the signal from the molecules with one Na^+ is half that from the fully occupied transporter (sr = 0.5 in Eq. 6), the normalized SPA signal is proportional to the sum of the fraction of molecules with two Na^+ ions bound and half the fraction of molecules with one Na^+ bound:

$$SPA_{2L} = K_x[L]^2 \Big/ \left\{1 + K_p[L] + K_x[L]^2\right\}$$

$$SPA_{1L} = 0.5K_p[\mathrm{L}] \Big/ \left\{1 + K_p[L] + K_x[L]^2\right\}.$$

Summing these two signals, we obtain

$$SPA_{total} = \left\{0.5K_p[\mathrm{L}] + K_x[L]^2\right\} \Big/ \left\{1 + K_p[L] + K_x[L]^2\right\}. \quad (8)$$

Eq. 8 assumes a maximum signal fraction of 1.0. Because of experimental and normalization errors, it is best to include a numerator multiplier SPA_{max}, which can also be fitted to the data. The value of the fitted SPA_{max} should remain close to 1.0.

Sodium binding by WT NIS SPA data

NIS is the key plasma membrane protein that mediates active I^- transport in the thyroid gland, the first step in the biosynthesis of the thyroid hormones, of which iodine is an essential constituent (Dai et al., 1996). NIS mutations have been linked to iodide transport defects, which lead to congenital hypothyroidism, deficit in the central nervous system development, and mental retardation if patients are not treated soon after birth (Dohán et al., 2002; De la Vieja et al., 2004, 2005; Paroder-Belenitsky et al., 2011; Li et al., 2013; Paroder et al., 2013; Portulano et al., 2014). NIS couples the inward "uphill" translocation of I^- against its electrochemical gradient to the inward "downhill" transport of Na^+ down its electrochemical gradient. NIS activity is electrogenic, with a 2:1 Na^+/I^- transport stoichiometry (Eskandari et al., 1997). It is able to accumulate iodide from serum concentrations orders of magnitude below its K_d. We have recently shown that at physiological Na^+

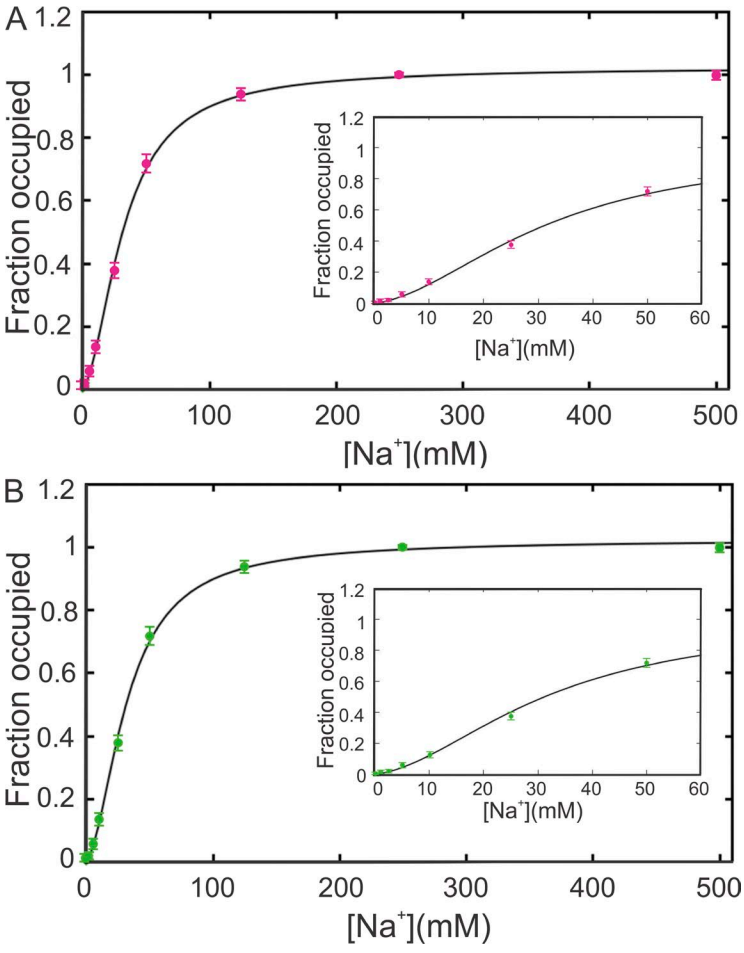

Figure 2. Na^+ binding by WT NIS. (A) SPA data for Na^+ binding by NIS fitted by Eq. 8. Data were collected and analyzed as described in Materials and methods. Values represent the means ± SE from three independent experiments performed in triplicate. The inset shows the fit at low [Na^+], where the cooperativity is more pronounced. (B) SPA data for Na^+ binding by WT NIS fitted using the Hill equation with a non-integer coefficient (Eq. 1). The data were fitted with a K_d of 31.8 mM and an n value of 1.74. The inset shows the fit at low [Na^+], where the cooperativity is more pronounced.

concentrations, ~79% of all NIS molecules have two Na^+ ions bound, and are therefore ready to bind and transport I^- (Nicola et al., 2014).

SPA experiments were performed to determine the affinity of Na^+ binding by NIS. NIS, like many other transporters in its family, has two independent binding sites for Na^+; both Na^+ ions that bind to NIS are used to transport I^-. The f_x values, obtained and normalized as detailed in Materials and methods, were fitted to Eq. 8 as a function of [Na^+] to obtain the K_p and K_x values (Fig. 2 A). The agreement between the calculated values (Fig. 2 A, continuous curve) and the experimental data is excellent $\left(rms_{resid} = \left\{\Sigma\left[f_{x,obs} - f_{x,calc}\right]^2 / [m-p]\right\}^{1/2} = 0.014\right)$ for f_x values in the range of 0–1.0; m is the number of experimental data points, and p is the number of parameters.

The extremes of the ranges provide examples of the combinations of affinities compatible with the data (Fig. 3, top and bottom). If $K_{d,A} = K_{d,B} = 225$ mM ($K_{d,X} = 1/K_{a,X}$) (Fig. 3, top), binding to a second site becomes highly favorable, with $K_{d,B}/\phi = 4.5$ mM (Fig. 3, bottom), a 50-fold enhancement. At the other extreme, when $K_{d,A}$ approaches 112.5 mM (i.e., $K_{d,B}$ approaches infinity), $K_{d,B}/\phi$ becomes 9.2 mM, corresponding to a very large enhancement. The actual values for NIS must fall within this range, somewhere between these two extremes.

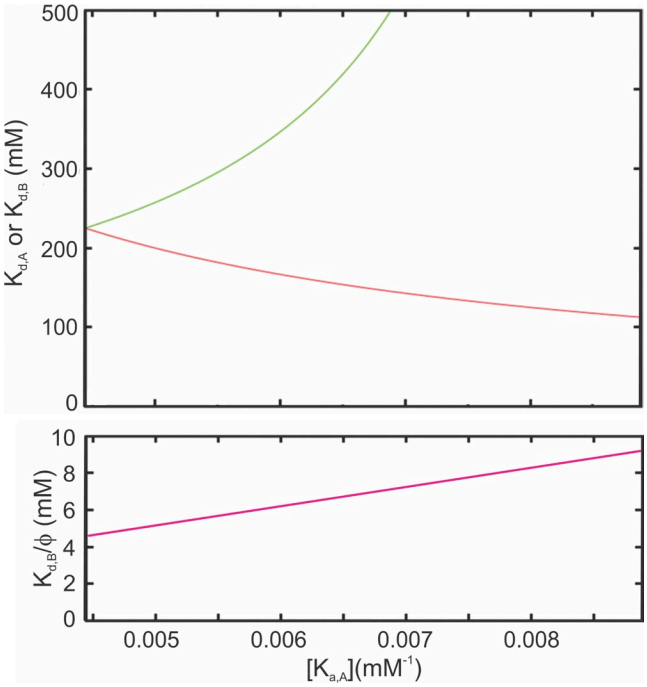

Figure 3. Ranges of dissociation constants for Na^+ binding by WT NIS. (Top) Dissociation constants for Na^+ binding by empty WT NIS—$K_{d,A}$ (red) and $K_{d,B}$ (green)—as a function of the allowed values for the association constant $K_{a,A}$. (Bottom) Enhanced dissociation constant for the second site when the first site is already occupied.

This analysis shows that the values of the dissociation constants for empty NIS, $K_{d,A}$, and $K_{d,B}$ (Fig. 3, top, left side) are compatible at one extreme, with both sites having the same affinity ($K_{d,A} = K_{d,B} = 225$ mM), and as the affinity of one of the sites (for example, site A) increases, that of the other must decrease to remain compatible with the experimental data. As $K_{d,A}$ decreases, the value of $K_{d,B}$ increases dramatically, approaching infinite as $K_{d,A}$ approaches 112.5 mM ($= 1/K_p$). However, because of the cooperativity, $K_{d,B}/\phi$ becomes highly favorable when site A is occupied (range of 4.6–9.2 mM; Fig. 3, bottom, left side). These values are very similar to those obtained by a statistical thermodynamic analysis of kinetic data ($K_{d,A} = 137$ mM and $K_{d,B} = 22.4$ mM) (Nicola et al., 2014).

It should be noted that the dissociation constant for the first site ($K_{d,A}$) and the enhanced dissociation constant for the second site ($K_{d,B}/\phi$) are always known within a factor of 2. Furthermore, if additional information becomes available—for example, from binding data for affinity mutants—the values of all three constants ($K_{d,A}$, $K_{d,B}$, and $K_{d,B}/\phi$) can be obtained.

The same data fitted to Eq. 1 (Fig. 2 B) gave a K_d value of 31.9 mM and an n of 1.74. This K_d is highly similar to the geometric mean of $K_{d,A}$ and $K_{d,B}/\phi$ (= 32.1 mM). Although the two equations yield fits of similar quality (see below), there is much more information in the values in Fig. 3 than in the two numbers obtained from fitting the data to the Hill equation.

Sodium binding by S353A/T354A NIS SPA data

The S353A/T354A NIS mutant was studied as a possible example of a NIS molecule that may bind a single Na^+ ion. Residues S353 and T354 were studied because the NIS mutant T354P causes iodide transport defect (Levy et al., 1998), and were identified as residues that are part of the coordination of one of the Na^+ ions (De la Vieja et al., 2007), like the corresponding residues in the bacterial leucine transporter LeuT (Yamashita et al., 2005). Alanine substitutions at NIS positions 353 and 354 abolish I^- transport (De la Vieja et al., 2007). To determine whether or not the lack of transport activity is caused by a lack of Na^+ binding, we generated the double mutant S353A/T354A and measured, using SPA, the binding of Na^+ to this NIS mutant. Surprisingly, the mutant binds two Na^+ ions, but the binding curve (Fig. 4 A) fails to show the positive cooperativity between the sites observed for the WT (Fig. 2 A).

The SPA data were fitted and analyzed using three different formalisms: (1) fit to Eq. 8 followed by the analysis proposed above (Figs. 4 A and 5); (2) fit to Hill equation (Eq. 1) (Fig. 4 B); and (3) fit assuming two independent sites (Fig. 4 C). The three formalisms fit the experimental data extremely well. Interestingly, the fit to Eq. 1 yields a single $K_d = 20.6$ mM and a Hill coefficient of 0.42. There is little information in these values besides a general $K_{d,50}$

and the indication of negative cooperativity ($n \leq 1$). Furthermore, the fact that the value of n is smaller than the minimum value (1/N = 0.5) expected for negative cooperativity (Abeliovich, 2005) suggests that Eq. 1 is not an appropriate model for ligand binding to this NIS mutant.

Analysis using the equations presented above yields a range of K_d values for the first site ($K_{d,A}$) between 0.99 and 1.98 mM (Fig. 5, top). For most of this range, the dissociation constant for binding Na^+ to site B when site A is not occupied remains small ($K_{d,B}$ = 4.75 mM at $K_{a,A}$ = 0.88 mM^{-1}; $K_{d,B}$ = 6.23 mM at $K_{a,A}$ = 0.85 mM^{-1}; Fig. 5), but it increases rapidly as $K_{a,A}$ approaches K_p. Negative cooperativity is manifested in binding to site B when site A is occupied ($K_{d,B}/\phi$; Fig. 5, bottom, cyan). In this situation, $K_{d,B}/\phi$, the dissociation constant for site B when site A is occupied, varies between 43.84 and 87.68 mM (Fig. 5, bottom, cyan). The values on the right side of the graph, 0.99 and 87.68 mM, are highly similar to those obtained by fitting two independent sites (0.90 and 80.48 mM). The similarity between these sets of values reflects the fact that, under these conditions, the two models describe similar situations: in both cases, site B starts binding after site A is substantially occupied. The analysis based on the formalism introduced here, however, describes other situations that are equally compatible with the data from SPA experiments. As mentioned before, analysis with the Hill equation provides much less information.

Equivalence of fitting by the two equations

It could be argued that the similarity between the quality of the fit using the Hill equation with a non-integer

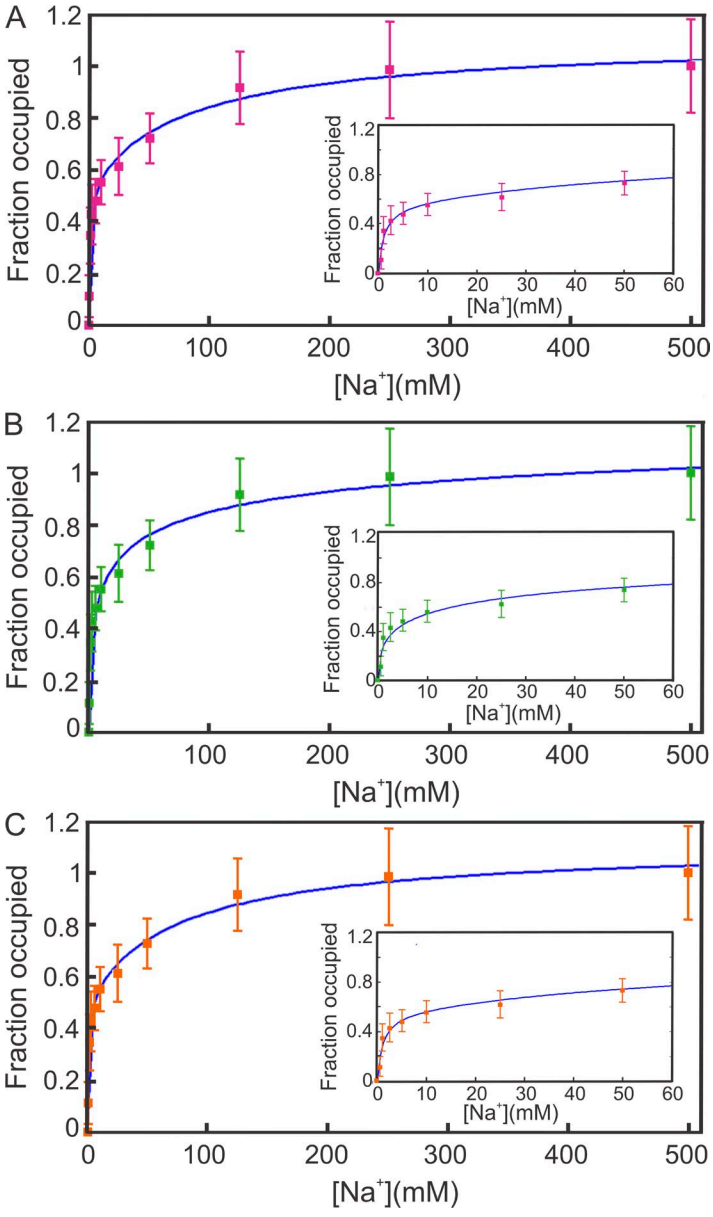

Figure 4. Na^+ binding by S353A/T354A NIS. (A) SPA data for Na^+ binding by S353A/T354A NIS fitted by Eq. 8. Data were collected and analyzed as described in Materials and methods. Values represent the means ± SE from two independent experiments performed in triplicate. The inset shows the fit at low [Na^+], where the cooperativity is more pronounced. (B) SPA data for Na^+ binding by S353A/T354A NIS fitted by the Hill equation with a non-integer coefficient (Eq. 1). The data were fitted with a K_d of 20.6 mM and an n value of 0.42. The inset shows the fit at low [Na^+], where the cooperativity is more pronounced. (C) SPA data for Na^+ binding by S353A/T354A NIS fitted for two independent sites. The data were fitted with a $K_{d,A}$ of 0.90 mM and a $K_{d,B}$ of 80.5 mM. The inset shows the fit at low [Na^+], where the effect of having two sites—one with high affinity and one with low affinity—is more pronounced.

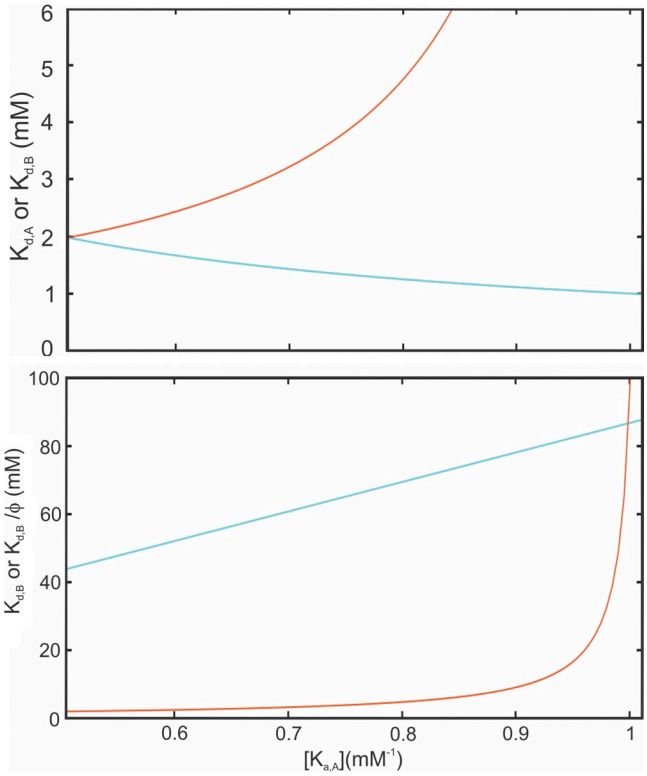

Figure 5. Ranges of dissociation constants for Na^+ binding by S353A/T354A NIS. (Top) Dissociation constants for Na^+ binding by empty NIS—$K_{d,A}$ (cyan) and $K_{d,B}$ (red)—as a function of the allowed values for the association constant $K_{a,A}$. $K_{d,A} = 1/K_{a,A}$ varies between 1.98 and 0.99 mM. (Bottom) $K_{d,B} = 1/(K_p - K_{a,A})$ (red) as a function of $K_{a,A}$ also begins at 1.98 mM ($K_p/2$; left side of graph) and increases slowly until approximately $K_{a,A} = 0.8$ mM^{-1}. As $K_{a,A}$ approaches K_p, $K_{a,B}$ approaches infinity (bottom graph, right). In contrast, although $K_{d,B}/\phi$ (cyan) begins at 43.78 mM when site A is occupied (negative cooperativity), it only increases to 87.68 mM when $K_{a,A} = K_p$ (right side of graph).

coefficient and that using the equations proposed here (i.e., similar rms_{resid} values) is a coincidence because of the particular values of the constants and n in the case of NIS. To test this possibility, we computed points with the Hill equation (Eq. 1) using values for n ranging from 1.7 to 1.9 and a K_d^n value of 0.001. The points in each individual curve were fitted by least squares using Eq. 8 (Fig. 6). The equation fits the calculated points with an rms_{resid} of <0.004, indicating that the two equations can fit the same data equally well.

Analysis of data obtained by other experimental methods

The formalism presented here can be used to analyze data obtained by other methods, for example, fluorescence (Reyes et al., 2013). In this case, f versus [L] data can be fitted by least squares to a version of Eq. 8 modified to take into account the fact that the signal with one L bound may not be half the signal when two L's are bound. The modified equation has the form

$$f_{total} = \left\{S_1 \cdot K_p[\mathrm{L}] + K_x[L]^2\right\} \Big/ \left\{1 + K_p[L] + K_x[L]^2\right\},$$

where S_1 is the fraction of the signal that occurs in response to binding of a single L (sr in Eq. 6). The value of S_1 can be estimated as part of the least-squares fit. The results obtained can be analyzed as described above. As mentioned earlier, these equations can be used when [L] ≈ L_{added}. In the case of fluorescence, this condition is met when [P] << K_d.

Summary of the approach

The equations for binding of a ligand to an allosteric macromolecule with two sites can be derived using three parameters, $K_{a,A}$, $K_{a,B}$, and ϕ (the enhancement of the affinity for binding the ligand to one of the sites that results from binding the ligand to the other site) (Hines et al., 2014), where $K_{a,A-B} = K_{a,B} \cdot \phi$ and $K_{a,B-A} = K_{a,A} \cdot \phi$ (Fig. 1). Fitting the experimental data to the three parameters in Eqs. 2a and 2b results in many combinations of parameters compatible with the data (Hines et al., 2014). The simple variable change shown in Eqs. 3 ($K_p = K_{a,A} + K_{a,B}$) and 4 ($K_x = K_{a,A} \cdot K_{a,B} \cdot \phi$) results in equations with only two parameters (K_p and K_x; Eqs. 5a and 5b) that fit the data much more stably. Once the values of K_p and K_x are obtained by least squares or

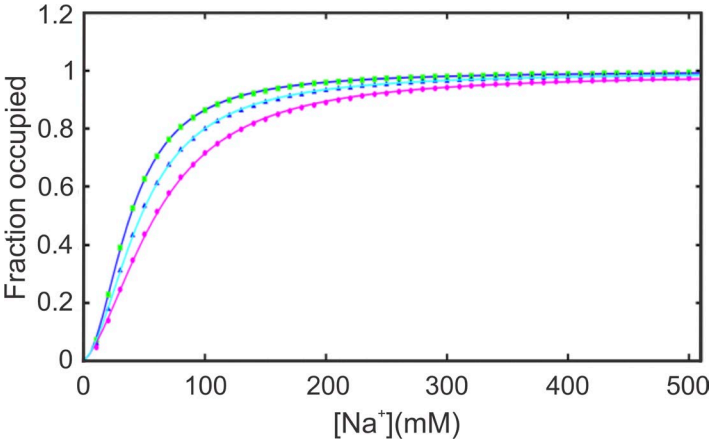

Figure 6. Fitting by Eq. 8 of points generated by Eq. 1. Points were generated using Eq. 1 with n values of 1.7 (mauve ovals), 1.8 (blue triangles), and 1.9 (green squares), and a K_d^n of 1,000 ($K_a^n = 0.001$). Each set of points was fitted using Eq. 8, resulting in the mauve, cyan, and blue curves, respectively.

other methods, $K_{a,A}$ and $K_{a,B}$ can be obtained as the two roots of a quadratic equation (Eq. 7a). Choosing A (arbitrarily) as the site with the higher affinity (the plus sign in Eq. 7a), the solutions are bound by the conditions $1/2\,K_p \le K_{a,A} \le K_p$ and $0 \le K_{a,B} \le 1/2\,K_p$. The binding affinity of site B for the ligand when site A is occupied can be obtained as $K_{a,B} \cdot \phi = K_x/K_{a,A}$. Therefore, even when $K_{a,B}$ approaches zero, $K_{d,B}/\phi = 1/K_{a,B} \cdot \phi$ remains finite. The results are a set of values for $K_{a,A}$, $K_{a,B}$, and $K_{a,B} \cdot \phi$ ($K_{d,A}$, $K_{d,B}$, and $K_{d,B}/\phi$), in which $K_{d,A}$ and $K_{d,B}/\phi$ are known within a factor of 2. This information, along with the fact that the values correspond to a well-defined binding reaction, makes the values obtained by this procedure ideally suited for establishing correlations with structural and computational results. Because $K_{a,A}$ and $K_{a,B} \cdot \phi$ are known within a factor of 2, the free energies of binding $\Delta G_{a,A}$ and $\Delta G_{a,A-B}$, calculated as $-RT\,ln\ K$, are known within ~0.4 Kcal/mol (= $RT\,ln\ 2$). Additional information can be obtained from the values of ϕ. The free energy of the interaction between the two sites ($\Delta g_{A,B}$) can be calculated as $-RT\,ln\ (\phi)$.

Conclusions

In summary, we present a method for analyzing binding data from a protein that binds the same ligand at two sites. In the case of a symmetric homodimer, the analysis provides values for the two binding constants: that for binding to the empty protein at either of the two sites ($K_{d,A}$ and $K_{d,B}$), and that for binding to the second site when the first site is occupied ($K_{d,B}/\phi$). In the case in which the two sites on the protein are different, the approach provides bounded pairs of possible values for the same constants. This information is missed when using the Hill equation with a non-integer coefficient. We tested the usefulness of the equations we propose by analyzing SPA data for NIS. In the case of WT NIS, the Hill equation fit gives a K_d of 31.8 mM and an n of 1.74 (Fig. 2 B). The approach presented here indicates that Na^+ binds to the first site with an affinity between 112.5 and 225 mM, and to the second site—once the first site is occupied—with an affinity between 9.2 and 4.6 mM. Although the square root of the product of the constants (32.2 mM) is highly similar to the Hill equation K_d, significant additional information is provided by the values obtained using the new approach. Thus, as opposed to the Hill equation, which provides n, an indication of cooperativity, and an overall K_d-like constant, the approach presented here provides narrowly bounded ranges of pairs of the values of all K_ds necessary to fully describe binding of the ligand. This formalism can also be used to analyze data of proteins that bind the same substrate at two binding sites.

We thank Drs. D. Leahy and A. Lau for critical reading of the manuscript and insightful discussions.

This study was supported by National Institutes of Health (grant DK-41544 to N. Carrasco).

The authors declare no competing financial interests.

Eduardo Rios served as editor.

Submitted: 15 January 2015
Accepted: 17 April 2015

REFERENCES

Abeliovich, H.. 2005. An empirical extremum principle for the Hill coefficient in ligand-protein interactions showing negative cooperativity. *Biophys. J.* 89:76–79.

Abramson, J., and E.M. Wright. 2009. Structure and function of Na^+-symporters with inverted repeats. *Curr. Opin. Struct. Biol.* 19: 425–432. http://dx.doi.org/10.1016/j.sbi.2009.06.002

Adair, G.S., A.V. Block, and H.J. Field. 1925. The hemoglobin system: VI. The oxygen dissociation curve of hemoglobin. *J. Biol. Chem.* 63:529–545.

Berry, J., and M. Price-Jones. 2005. Measurement of radioligand binding by scintillation proximity assay. *Methods Mol. Biol.* 306:121–137.

Caplan, D.A., J.O. Subbotina, and S.Y. Noskov. 2008. Molecular mechanism of ion-ion and ion-substrate coupling in the Na^+-dependent leucine transporter LeuT. *Biophys. J.* 95:4613–4621. http://dx.doi.org/10.1529/biophysj.108.139741

Dahlquist, F.W. 1978. The meaning of Scatchard and Hill plots. *Methods Enzymol.* 48:270–299. http://dx.doi.org/10.1016/S0076-6879(78)48015-2

Dai, G., O. Levy, and N. Carrasco. 1996. Cloning and characterization of the thyroid iodide transporter. *Nature.* 379:458–460. http://dx.doi.org/10.1038/379458a0

De la Vieja, A., C.S. Ginter, and N. Carrasco. 2004. The Q267E mutation in the sodium/iodide symporter (NIS) causes congenital iodide transport defect (ITD) by decreasing the NIS turnover number. *J. Cell Sci.* 117:677–687. http://dx.doi.org/10.1242/jcs.00898

De la Vieja, A., C.S. Ginter, and N. Carrasco. 2005. Molecular analysis of a congenital iodide transport defect: G543E impairs maturation and trafficking of the Na^+/I^- symporter. *Mol. Endocrinol.* 19:2847–2858. http://dx.doi.org/10.1210/me.2005-0162

De la Vieja, A., M.D. Reed, C.S. Ginter, and N. Carrasco. 2007. Amino acid residues in transmembrane segment IX of the Na^+/I^- symporter play a role in its Na^+ dependence and are critical for transport activity. *J. Biol. Chem.* 282:25290–25298. http://dx.doi.org/10.1074/jbc.M700147200

Dohán, O., M.V. Gavrielides, C. Ginter, L.M. Amzel, and N. Carrasco. 2002. Na^+/I^- symporter activity requires a small and uncharged amino acid residue at position 395. *Mol. Endocrinol.* 16:1893–1902. http://dx.doi.org/10.1210/me.2002-0071

Eskandari, S., D.D. Loo, G. Dai, O. Levy, E.M. Wright, and N. Carrasco. 1997. Thyroid Na^+/I^- symporter. Mechanism, stoichiometry, and specificity. *J. Biol. Chem.* 272:27230–27238. http://dx.doi.org/10.1074/jbc.272.43.27230

Fotiadis, D., Y. Kanai, and M. Palacín. 2013. The SLC3 and SLC7 families of amino acid transporters. *Mol. Aspects Med.* 34:139–158. http://dx.doi.org/10.1016/j.mam.2012.10.007

Goutelle, S., M. Maurin, F. Rougier, X. Barbaut, L. Bourguignon, M. Ducher, and P. Maire. 2008. The Hill equation: a review of its capabilities in pharmacological modelling. *Fundam. Clin. Pharmacol.* 22:633–648. http://dx.doi.org/10.1111/j.1472-8206.2008.00633.x

Harder, D., and D. Fotiadis. 2012. Measuring substrate binding and affinity of purified membrane transport proteins using the scintillation proximity assay. *Nat. Protoc.* 7:1569–1578. http://dx.doi.org/10.1038/nprot.2012.090

Hill, A.V. 1910. Proceedings of the Physiological Society: January 22, 1910. The possible effects of the aggregation of the molecules of hæmoglobin on its dissociation curves. *J. Physiol.* 40:iv–vii. http://dx.doi.org/10.1113/jphysiol.1910.sp001386

Hill, A.V. 1913. The Combinations of haemoglobin with oxygen and with carbon monoxide. I. *Biochem. J.* 7:471–480.

Hines, K.E., T.R. Middendorf, and R.W. Aldrich. 2014. Determination of parameter identifiability in nonlinear biophysical models: A Bayesian approach. *J. Gen. Physiol.* 143:401–416. http://dx.doi.org/10.1085/jgp.201311116

Ho, A.L., R.K. Grewal, R. Leboeuf, E.J. Sherman, D.G. Pfister, D. Deandreis, K.S. Pentlow, P.B. Zanzonico, S. Haque, S. Gavane, et al. 2013. Selumetinib-enhanced radioiodine uptake in advanced thyroid cancer. *N. Engl. J. Med.* 368:623–632. http://dx.doi.org/10.1056/NEJMoa1209288

Khafizov, K., C. Perez, C. Koshy, M. Quick, K. Fendler, C. Ziegler, and L.R. Forrest. 2012. Investigation of the sodium-binding sites in the sodium-coupled betaine transporter BetP. *Proc. Natl. Acad. Sci. USA.* 109:E3035–E3044. http://dx.doi.org/10.1073/pnas.1209039109

Klutz, K., M.J. Willhauck, N. Wunderlich, C. Zach, M. Anton, R. Senekowitsch-Schmidtke, B. Göke, and C. Spitzweg. 2011. Sodium iodide symporter (NIS)-mediated radionuclide ((131)I, (188)Re) therapy of liver cancer after transcriptionally targeted intratumoral in vivo NIS gene delivery. *Hum. Gene Ther.* 22:1403–1412. http://dx.doi.org/10.1089/hum.2010.158

Levy, O., C.S. Ginter, A. De la Vieja, D. Levy, and N. Carrasco. 1998. Identification of a structural requirement for thyroid Na^+/I^- symporter (NIS) function from analysis of a mutation that causes human congenital hypothyroidism. *FEBS Lett.* 429:36–40. http://dx.doi.org/10.1016/S0014-5793(98)00522-5

Li, W., J.P. Nicola, L.M. Amzel, and N. Carrasco. 2013. Asn441 plays a key role in folding and function of the Na^+/I^- symporter (NIS). *FASEB J.* 27:3229–3238. http://dx.doi.org/10.1096/fj.13-229138

Nicola, J.P., N. Carrasco, and L.M. Amzel. 2014. Physiological sodium concentrations enhance the iodide affinity of the Na^+/I^- symporter. *Nat. Commun.* 5:3948. http://dx.doi.org/10.1038/ncomms4948

Paroder, V., J.P. Nicola, C.S. Ginter, and N. Carrasco. 2013. The iodide-transport-defect-causing mutation R124H: a δ-amino group at position 124 is critical for maturation and trafficking of the Na^+/I^- symporter. *J. Cell Sci.* 126:3305–3313. http://dx.doi.org/10.1242/jcs.120246

Paroder-Belenitsky, M., M.J. Maestas, O. Dohán, J.P. Nicola, A. Reyna-Neyra, A. Follenzi, E. Dadachova, S. Eskandari, L.M. Amzel, and N. Carrasco. 2011. Mechanism of anion selectivity and stoichiometry of the Na^+/I^- symporter (NIS). *Proc. Natl. Acad. Sci. USA.* 108:17933–17938. http://dx.doi.org/10.1073/pnas.1108278108

Pirch, T., M. Quick, M. Nietschke, M. Langkamp, and H. Jung. 2002. Sites important for Na^+ and substrate binding in the Na^+/proline transporter of *Escherichia coli*, a member of the Na^+/solute symporter family. *J. Biol. Chem.* 277:8790–8796. http://dx.doi.org/10.1074/jbc.M111008200

Portulano, C., M. Paroder-Belenitsky, and N. Carrasco. 2014. The Na^+/I^- symporter (NIS): Mechanism and medical impact. *Endocr. Rev.* 35:106–149. http://dx.doi.org/10.1210/er.2012-1036

Quick, M., and J.A. Javitch. 2007. Monitoring the function of membrane transport proteins in detergent-solubilized form. *Proc. Natl. Acad. Sci. USA.* 104:3603–3608. http://dx.doi.org/10.1073/pnas.0609573104

Reyes, N., S. Oh, and O. Boudker. 2013. Binding thermodynamics of a glutamate transporter homolog. *Nat. Struct. Mol. Biol.* 20:634–640. http://dx.doi.org/10.1038/nsmb.2548

Shi, L., M. Quick, Y. Zhao, H. Weinstein, and J.A. Javitch. 2008. The mechanism of a neurotransmitter:sodium symporter—inward release of Na^+ and substrate is triggered by substrate in a second binding site. *Mol. Cell.* 30:667–677. http://dx.doi.org/10.1016/j.molcel.2008.05.008

Weiss, J.N. 1997. The Hill equation revisited: uses and misuses. *FASEB J.* 11:835–841.

Wright, E.M. 2013. Glucose transport families SLC5 and SLC50. *Mol. Aspects Med.* 34:183–196. http://dx.doi.org/10.1016/j.mam.2012.11.002

Yamashita, A., S.K. Singh, T. Kawate, Y. Jin, and E. Gouaux. 2005. Crystal structure of a bacterial homologue of Na^+/Cl^--dependent neurotransmitter transporters. *Nature.* 437:215–223. http://dx.doi.org/10.1038/nature03978

Zhou, X., E.J. Levin, Y. Pan, J.G. McCoy, R. Sharma, B. Kloss, R. Bruni, M. Quick, and M. Zhou. 2014. Structural basis of the alternating-access mechanism in a bile acid transporter. *Nature.* 505:569–573. http://dx.doi.org/10.1038/nature12811